The Journal of Experimental Biology **199**, 775–791 (1996)
Printed in Great Britain © The Company of Biologists Limited 1996
JEB9985

NOVEL DUAL INNERVATION OF A LARVAL PROLEG MUSCLE BY TWO SIMILAR MOTONEURONS IN THE TOBACCO HORNWORM *MANDUCA SEXTA*

DAVID J. SANDSTROM[1,*] AND JANIS C. WEEKS[2]

[1]*Graduate Group in Neurobiology, University of California at Berkeley, Berkeley, CA 94720, USA* and [2]*Institute of Neuroscience, University of Oregon, Eugene, OR 97403-1254, USA*

Accepted 8 December 1995

Summary

In *Manduca sexta*, the accessory planta retractor muscle (APRM), which retracts the larval proleg, is innervated by two excitatory motoneurons, the accessory planta retractor motoneurons (APRs). These muscles and motoneurons have been the focus of a number of developmental and behavioral studies. The present study investigated properties of the pair of APRs that innervate each APRM and determined their pattern of innervation of APRM fibers. Members of APR pairs could not be distinguished by their anatomical or electrical properties (resting membrane potential, input resistance and spike threshold). Spontaneous synaptic inputs to members of APR pairs were highly correlated, whereas spontaneous synaptic inputs to APRs and functionally dissimilar motoneurons were not well correlated. Synaptic inputs from identified mechanosensory neurons and interneurons to the two APRs were qualitatively similar, but the magnitude of the response to sensory stimulation sometimes differed within a pair. Both APRs produced large, rapidly rising excitatory junction potentials in APRM fibers. Within the APRM, some fibers were singly innervated by one or the other APR while the remaining fibers were dually innervated by both APRs. In dually innervated fibers, the motor terminals of the two APRs were spatially segregated. This innervation pattern appears to be unique among insects and shares some properties with the innervation of vertebrate muscle.

Key words: motoneuron, sensory neuron, moth, neuromuscular junction, *Manduca sexta*, synapse, muscle, proleg.

Introduction

A major goal of neurobiology is to understand how the properties of individual neurons contribute to behavior. For a neuron to perform properly in a neural circuit, it must have suitable electrical properties, receive appropriate synaptic inputs and make the correct output connections. The study of simple behavior patterns, such as sensory-evoked reflexes, has allowed the roles of specific neurons in the generation of behavior to be characterized in ever-increasing detail. This approach has been used to investigate various aspects of nervous system function, including sensorimotor integration, behavioral plasticity and the hormonal modulation of behavior patterns (e.g. Wine and Krasne, 1982; Byrne *et al.* 1990; Levine and Weeks, 1990; Burrows, 1992). These lines of research have demonstrated the importance of understanding the detailed properties of neurons in order to understand how a circuit generates a particular type of behavior. The goal of this approach is to understand animal behavior at the level of the underlying cellular components and the synaptic connections among them.

The proleg neuromuscular system of *Manduca sexta* has proved useful for investigating how individual neurons contribute to behavior. Prolegs are the primary locomotory appendages of *M. sexta* caterpillars, consisting of paired evaginations of the ventral abdominal body wall. Each proleg bears an array of crochets, which are curved hooks used to attach to the substratum. Prolegs are capable of retraction (withdrawal), extension and adduction movements. Withdrawal occurs by contraction of proleg retractor muscles (see below), whereas extension occurs passively by hydrostatic pressure when the retractor muscles relax (Weeks and Truman, 1984*a*). Adductor muscles move the prolegs towards the ventral midline (Weeks and Ernst-Utzschneider, 1989), allowing pairs of prolegs to grasp objects between them. The prolegs participate in many types of larval behavior, including a withdrawal reflex evoked by stimulation of mechanosensory hairs on the proleg tip (reviewed in Weeks *et al.* 1996), pre-ecdysis (cuticle loosening) behavior (Miles and Weeks, 1991; Novicki and Weeks, 1993), ecdysis (cuticle shedding) behavior (Weeks and Truman, 1984*a*) and crawling.

Each proleg has several retractor muscles, including the accessory planta retractor muscle (APRM; Weeks and Truman, 1984*a*). This muscle, which retracts the proximal portion of the

*Present address: ARL-Division of Neurobiology, 611 Gould Simpson Building, University of Arizona, Tucson, AZ 85721, USA.

proleg (see Fig. 1A), was the focus of the present study. APRMs are present bilaterally in proleg-bearing abdominal segments 3–6 (A3–A6; see Fig. 1A); apparent homologs of APRM also occur in segments A1 and A2, which do not bear prolegs (Weeks and Ernst-Utzschneider, 1989). Each APRM is innervated by two excitatory motoneurons, the APRs (Weeks and Truman, 1984*a*), which are located in the ganglion of the same segment ipsilateral to the muscle that they innervate (see Fig. 1B). In contrast, single excitatory motoneurons appear to innervate other larval *M. sexta* muscles (e.g. Levine and Truman, 1985; Weeks and Truman, 1985; Thorn and Truman, 1989; Miles and Weeks, 1991). Dual innervation of the APRM was inferred from the observation that intracellular stimulation of either member of an APR pair caused the ipsilateral APRM to contract (Weeks and Truman, 1984*a*). The terms 'the two APRs,' 'both APRs' or 'APR pairs' are used below when referring to the pair of APRs that innervate the same APRM. The apparent homologs of APRM in segments A1 and A2 are innervated by a pair of motoneurons that appear to be homologous to the APRs (Weeks and Ernst-Utzschneider, 1989).

The assumption made in previous studies (e.g. Weeks and Ernst-Utzschneider, 1989; Sandstrom and Weeks, 1991*a*; Weeks *et al.* 1992, 1993; Streichert and Weeks, 1994, 1995; Weeks and Davidson, 1994), that the two APRs are equivalent, had not been tested explicitly. Differences in the anatomy of the APRs and their intrinsic electrical properties, synaptic inputs, activation thresholds and/or output connections onto muscle fibers could have behavioral consequences and could also affect the interpretation of other studies. Measurement of these characteristics in the present study showed that members of APR pairs were indistinguishable by most criteria except for small but consistent differences in their responses to sensory input. No functional consequences of this difference were apparent. One novel finding was the innervation pattern of the APRM by the APRs: some APRM fibers were innervated by one or the other APR, while the remaining fibers received spatially segregated input from both APRs. To our knowledge, this form of multiple innervation has not been described previously in insects and may possibly result from competition between the two APRs that innervate each APRM. Some of these results have appeared in abstract form (Sandstrom and Weeks, 1991*b*).

Materials and methods

Experimental animals

Larval tobacco hornworms [*Manduca sexta* (Johannson); Sphingidae] were reared on an artificial diet (modified from Bell and Joachim, 1978) under a 17 h:7 h light:dark cycle and 27 °C:25 °C thermoperiod. Male larvae were used on the first to the fourth day of the fifth (final) instar (Weeks and Truman, 1985).

Electrophysiological techniques

Insects were anesthetized and dissected as described previously (Sandstrom and Weeks, 1991*a*). A ganglion from segment A3, A4 or A5 was removed, treated with collagenase–dispase (Boehringer Mannheim, Indianapolis, IN, USA) and desheathed (Weeks and Jacobs, 1987). Desheathed ganglia were bathed in a physiological saline containing (in $mmol\,l^{-1}$): NaCl, 140; KCl, 5; $CaCl_2$, 4; glucose, 28; Hepes, 5; pH 7.4 (Trimmer and Weeks, 1989). Activity in segmental nerves (see below) was monitored with glass-tipped suction electrodes, using differential, high-gain, a.c.-coupled preamplifiers. Electrophysiological data were recorded on magnetic tape at $3.75\,in\,s^{-1}$ (Vetter Instruments, Rebersburg, PA). Some data were later digitized and analyzed on a PC equipped with data analysis software (Computerscope, R.C. Electronics, Santa Barbara, CA, USA) or exported as ASCII files to other analysis programs (see below).

Intracellular recordings were made with thin-walled borosilicate electrodes filled with $2\,mol\,l^{-1}$ potassium acetate (25–35 MΩ). Some electrodes (see below) were beveled to 10–15 MΩ in a spinning slurry of 400 grit silicon carbide. Motoneurons were visualized and identified as described previously (e.g. Sandstrom and Weeks, 1991*a*). Intracellular recordings were amplified using high input impedance amplifiers (model 8800 Total Clamp, Dagan Instruments, Minneapolis, MN, USA). The discontinuous single-electrode current-clamp (SEC) mode of the Dagan amplifier was used to measure membrane potential (V_m) accurately while injecting current into APRs. Switching frequency was approximately 5 kHz, with a 50 % duty cycle (with beveled electrodes). Resting V_m was measured as the mean of two single points from two signal-averaged (10 sweeps) measurements from each APR. Spike threshold, input resistance (R_{in}) and membrane time constant (τ_m) were measured while holding V_m at −60 mV in SEC mode. Spike threshold was measured at the inflection of the first action potential (spike) during a ramp of depolarizing current (500 ms, 0.5 nA peak) generated by a Tektronix 26G1 ramp/rate generator controlling the internal current source of the Dagan 8800. R_{in} was measured by injecting square current pulses (500 ms, −0.1 to −1.2 nA) at 0.5 Hz. Three voltage responses were averaged for each current amplitude, and R_{in} was calculated from the slope of the *I*/*V* relationship. τ_m (τ_0 in Rall, 1969) was determined by fitting an exponential function to voltage responses during *I*/*V* measurements (Sigmaplot, Jandel Corp., Corte Madera, CA, USA). APRs that exhibited a progressive decrease in V_m, R_{in} or spike amplitude during intracellular recording were excluded from the study. APR pairs were excluded if electrode drift (measured as the difference from 0 mV when the electrode was withdrawn) produced an error of more than 5.0 mV between the two motoneurons.

Synaptic input from planta hair (PH) sensory neurons to APR pairs was measured by electrically stimulating the branch of the ventral nerve (VN) containing the PH sensory neuron axons (VN_{AABr3}; Jacobs and Weeks, 1990; Streichert and Weeks, 1995). VN_{AABr3} was stimulated with 0.1 ms square pulses (Grass S88 and SIU5, Grass Instruments Co., Quincy, MA, USA) *via* a suction electrode. Stimulus voltage was adjusted to exceed slightly that which produced a maximal

response recorded *en passant* in VN near the ganglion. APRs were held at −60 mV in SEC mode and 4–8 VN_{AABr3} stimuli were delivered at a rate of 1 every 30 s; by averaging only the second response to the last response, the interstimulus interval was the same for all trials. When two APRs were recorded simultaneously, the sample-and-hold circuits of two Dagan 8800s were synchronized. Synaptic connections from an identified interneuron (IN-703) (Sandstrom and Weeks, 1991*a*) to APR pairs were measured by impaling IN-703 and sequentially impaling the two APRs. Excitatory postsynaptic potentials (EPSPs) were signal-averaged (20 sweeps) using Computerscope.

Spontaneous synaptic inputs to members of APR pairs, and to APR and an identified motoneuron (MN-1) (Levine and Truman, 1985), were recorded during simultaneous impalements in isolated whole nerve cords. MN-1 was identified by its soma position and the presence of a time-locked spike in the appropriate nerve branch (Levine and Truman, 1985). In some cases, a small amount of hyperpolarizing current (less than 0.25 nA) was injected to prevent spontaneous firing in MN-1. For statistical analysis (see Results), 3.2 s of data from each pair of motoneurons were digitized at 10 kHz and exported to Sigmaplot for analysis.

Muscle recordings

An APRM, and the ganglion that innervated it (connected *via* the lateral branch of the ventral nerve, VN_L), were removed and the muscle was pinned in a dish by its cuticular attachment points at the approximate *in vivo* length. Muscle preparations were superfused with the saline used for desheathed ganglia, which reduced regenerative muscle currents and contractions (see Results). The electrical properties of the APRM remained stable over hours of recording.

APRM fibers were impaled with intracellular electrodes (see above) and excitatory junction potentials (EJPs) from one or both APRs were evoked by injecting depolarizing current into the APR(s) or by stimulating VN_L with brief current pulses delivered *via* a suction electrode. Both methods produced the same results. EJPs were recorded at interstimulus intervals greater than 30 s during sequential impalements at multiple sites along each APRM fiber. Recording sites were marked on a map of the muscle drawn with a *camera lucida* attachment on a dissecting microscope. Each preparation was subsequently fixed in 70 % ethanol for 20–30 min, and the APRM was teased apart to determine the number of fibers and their positions. Muscle fibers having any physical continuity were counted as a single fiber.

The coupling coefficients of the muscle fibers, R_{in}, the length constant (λ) and the EJP reversal potential (E_{rev}) were measured using two or three electrodes. A beveled electrode was used to inject current while one or more unbeveled electrodes measured the resulting potentials. Electrical coupling between APRM fibers was determined by injecting current into a fiber, recording the voltage nearby in the same fiber with a second electrode, and recording the V_m of an adjacent fiber with a third electrode. Coupling coefficients were calculated by dividing the voltage deflection in the adjacent fiber by that at the site of current injection. R_{in} was measured by injecting 500 ms current steps from −1000 to +500 nA and recording the voltage nearby with a second electrode. To measure λ, current was injected at one site on a muscle fiber and voltage was measured nearby in the same fiber with a second electrode (V_0) and at measured distances along the muscle fiber with a third electrode (V_x). λ was calculated by fitting a plot of V_x/V_0 *versus* distance to the equation:

$$V_x/V_0 = [\cosh(L - x/\lambda)]/\cosh(L/\lambda),$$

where L is the length of the fiber and x is the distance between V_0 and V_x (Jack *et al.* 1975; Dietmer, 1977). The E_{rev} of EJPs was measured by evoking EJPs while injecting 500 ms current steps from −500 to +300 nA at the recording site. E_{rev} was extrapolated from the regression line of the plot of V_{EJP} *versus* V_m.

Semi-intact sensory preparations

A semi-intact preparation consisting of a ganglion and a portion of body wall that included the planta (distal tip of the proleg), the APRM and sometimes the principal planta retractor muscle (PPRM) was used to measure motoneuron responses to sensory stimulation (Weeks and Jacobs, 1987). The proleg tip and PH array projected above the level of the saline. PHs were deflected manually while EJPs were recorded from muscle fibers.

Histological techniques

After recording physiological data, some APRs were reimpaled with an electrode containing 2–5 % $CoCl_2$. The cobalt was ionophoresed, the stain was intensified and ganglia were mounted as described previously (Sandstrom and Weeks, 1991*a*). Stained APRs were drawn with a *camera lucida* attachment on a compound microscope. For transverse sections, ganglia were removed from slides, embedded in plastic and sectioned as described previously (Sandstrom and Weeks, 1991*a*).

To observe the dendritic arborizations of both APRs in the same hemiganglion, one was injected with 5 % $CoCl_2$ and the other with 5 % $NiCl_2$. Nickel-stained cells were dark blue and cobalt-stained cells were orange-red. APRs were impaled simultaneously with beveled electrodes containing the solutions, which were ionophoresed for 10 min using +20 nA, 500 ms pulses at 1 Hz. The stain was immediately precipitated for 10 min in saline containing 5 drop ml^{-1} of saturated ethanolic rubeanic acid (dithio-oxamide, Sigma Chemical Co., St Louis, MO, USA; Quicke and Brace, 1979). Ganglia were fixed for 1 h in Carnoy's fixative, transferred to 70 % ethanol, rehydrated and treated with 0.5 % Triton X-100 (Sigma) for 10 min, dehydrated in an ethanol series, cleared in methyl salicylate, and mounted whole in Canada Balsam.

APR terminals on the APRM were stained anterogradely in young fifth-instar larvae, whose smaller size reduced diffusion time. To visualize the terminals of both APRs, the APRM and

the associated VN (cut adjacent to the ganglion) were dissected and placed in a chamber with two wells. The APRM was placed in a well containing physiological saline (Weeks and Truman, 1984*b*) while the severed VN was placed in a well containing distilled water, which was replaced after 5 min with 2 % $CoCl_2$. Cobalt was allowed to diffuse towards the APRM for 1–3 days. The motor terminals of individual APRs were visualized by impaling an APR with an electrode containing 5 % $CoCl_2$ and ionophoresing cobalt with 500 ms, +10 nA pulses at 1 Hz for 10–15 min. The ganglion and APRM were kept at 4 °C for 4.5–18 h (9 h was optimal). All tissue was subsequently processed as in Sandstrom and Weeks (1991*a*). Preparations were excluded if motor axons ended abruptly or the staining faded away gradually rather than ending in distinct terminals on the muscle.

Statistics

All values are mean ± standard error. Differences between means were compared using two-tailed paired or independent *t*-tests, differences between experimental and expected means were compared by *z*-scores, and distributions were tested for significance by chi-square analysis (Snedecor and Cochran, 1980). Coefficients of correlation (*r*-values) were used to test for correlations within a distribution and pairs of *r*-values were compared using a *t*-test for *r*-values (Walker and Lev, 1953).

Results

Anatomy of the APRs

In the abdominal proleg-bearing segments (A3–A6), the APRM has a dorsal insertion point just posterior to the spiracle and a ventral insertion point on the lateral surface of the planta (Fig. 1A). The somata of the two APRs that innervate each APRM are located anterolaterally on the ventral surface of the ganglion of the same segment (Fig. 1B) and their axons reach the APRM *via* the ipsilateral VN_L (Weeks and Truman, 1984*a*). The soma of one APR is typically more anterior than that of the other, with a variable distance between the two (Fig. 1B). For some experiments, APRs were identified by soma position (anterior or posterior) and data from the two groups were compared. Soma position was correlated with some but not all of the properties of the APRs (see below). In other experiments, we made paired comparisons of the properties of the two APRs that innervated a particular APRM, without regard for soma position.

The major anatomical features of the dendritic arborizations of the two APRs, revealed by intracellular cobalt injection, were similar (Fig. 1C,D). All APRs had arborizations ipsilateral to their cell body, concentrated in the anterior quadrant of the neuropil (Fig. 1C). Most processes were located in dorsal and lateral neuropil (Fig. 1D), which is typical of insect motoneurons (e.g. Kutsch and Schneider, 1987; Weeks and Jacobs, 1987; Miles and Weeks, 1991). The APRs also have a characteristic projection to ventral neuropil where the sensory neurons that innervate PHs project (partially apparent in Fig. 1Di; Weeks and Jacobs, 1987; Peterson and Weeks, 1988). Both anterior (*N*=22) and posterior (*N*=14) APRs had ventral dendritic projections.

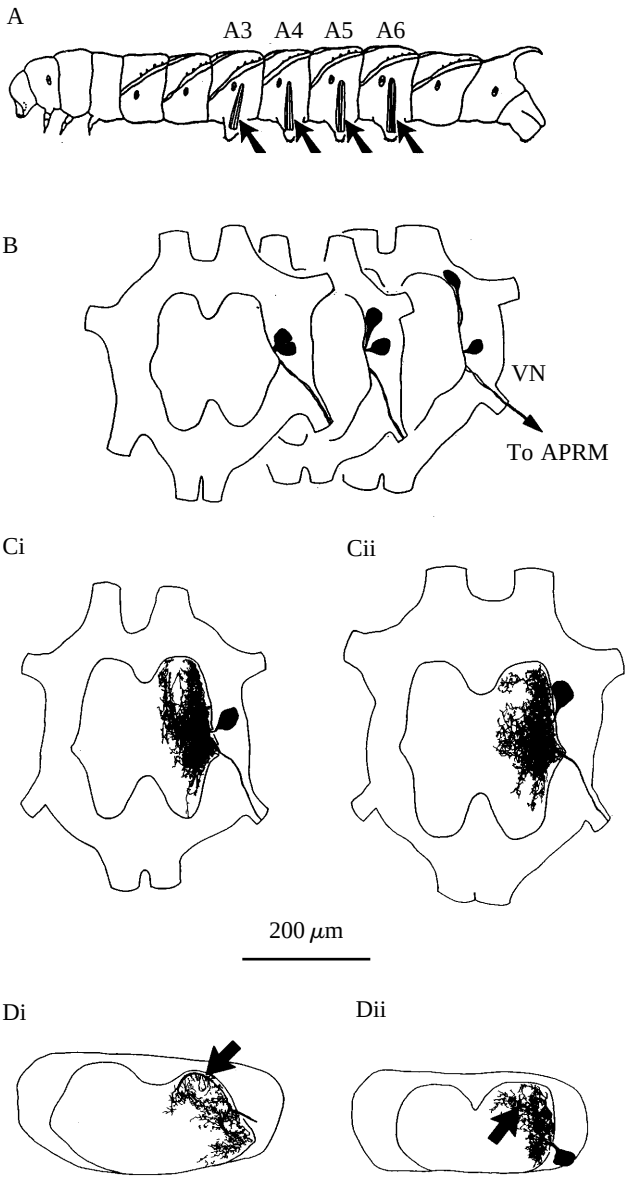

Fig. 1. The accessory planta retractor motoneuron (APR) and muscle (APRM). (A) *Manduca sexta* caterpillar, anterior to left. The proleg-bearing abdominal segments (A3–A6) are labeled and the left APRM in each segment is indicated (arrows). In B–D, APRs were stained intracellularly with cobalt. (B) Drawings of ganglia in which both APRs of a pair were stained: somata, primary neurites and axons are shown while dendrites in the neuropil (double ovoid) are not drawn. The three examples (shown in partial overlap) illustrate the range of positions of the somata of the APRs. Anterior is up. VN, ventral nerve. (C) *Camera lucida* drawings illustrating APR dendritic morphology: Ci, APR with a posterior cell body; Cii, APR with an anterior cell body. Anterior is up. (D) Drawings of single transverse sections of APRs (dorsal is up): Di, APR with a dorsal neurite (arrow; soma not in plane of section); Dii, APR with a neurite in intermediate neuropil (arrow; same APR as in Cii). The full extent of the ventral projection of the APRs is not shown. The scale bar refers to B–D.

One anatomical feature did vary among APRs. All APRs

sent processes to dorsomedial neuropil, but some projected to this region *via* a stout, extremely dorsally located neurite (Fig. 1Di), whereas others lacked the prominent dorsal neurite and projected *via* a neurite in the intermediate region of the neuropil (Fig. 1Dii). We tested the hypothesis that, within each pair of APRs, one APR had a dorsal neurite and one APR had an intermediate neurite, by differentially staining members of APRs pairs with nickel and cobalt (see Materials and methods). Of 17 pairs, 10 pairs had one APR of each type, six pairs had two APRs with dorsal neurites and one pair had two APRs with intermediate neurites. Therefore, neurite position did not exhibit a consistent pattern in APR pairs. When cell body position was compared with neurite position, anterior APRs were unbiased with respect to neurite position (52 % dorsal *versus* 48 % intermediate; chi-square, $P>0.10$; $N=44$), whereas posterior APRs preferentially had dorsal neurites (83 % dorsal *versus* 17 % intermediate; chi-square, $P<0.01$; $N=36$).

Electrical properties of the APRs

Resting V_m, spike threshold, R_{in} and τ_m were measured in 10 pairs of APRs, recorded sequentially (Fig. 2; Table 1). Fig. 2 illustrates data from a single pair of APRs. Both APRs had similar values of resting V_m and spike threshold (Fig. 2A), responded similarly to hyperpolarizing current steps (Fig. 2B), and had nearly identical *I*/*V* plots and R_{in} values (Fig. 2C). The membrane time constants of the two APRs, determined by fitting exponential curves to the charging portions of the voltage waveforms (Fig. 2B), were also nearly identical: τ_m was 29.2 ms for the anterior APR and 30.1 ms for the posterior APR. Table 1 shows that similar results were obtained for all APR pairs tested ($N=10$): there were no significant differences in any measured electrical properties. For comparison, Table 1 also shows data for the principal planta retractor motoneuron, PPR (Trimmer and Weeks, 1989, 1993). Differences between PPR and the APRs in V_m, spike threshold and R_{in} suggested that PPR should be more excitable than the APRs (see below).

Synaptic inputs to the APRs

We investigated synaptic inputs to APR pairs from sensory neurons that innervate planta hairs (PHs) on the proleg tip (Weeks and Jacobs, 1987; Peterson and Weeks, 1988) and from an identified interneuron, IN-703 (Sandstrom and Weeks, 1991*a*). We also examined spontaneous synaptic inputs from unidentified sources.

In larvae, deflection of PHs evokes proleg withdrawal, due to direct and indirect excitatory synaptic connections from PH sensory neurons to PPR and the APRs (reviewed in Weeks *et al.* 1996). Electrical stimulation of the proleg sensory nerve, VN_{AABr3}, activates the PH sensory neurons and evokes a synaptic depolarization in proleg motoneurons, termed the compound excitatory postsynaptic potential (cEPSP; Streichert and Weeks, 1995). We stimulated VN_{AABr3} with single shocks once every 30 s (Fig. 3A) and recorded the responses of APR pairs simultaneously ($N=5$ pairs) or sequentially ($N=7$ pairs). APRs were held at −60 mV (SEC mode) to standardize V_m.

The data were analyzed in two ways. First, for each APR, we determined the mean cEPSP amplitude and number of spikes produced, averaged over multiple VN_{AABr3} stimulation trials (see Materials and methods). For the entire group of APRs ($N=24$), mean cEPSP amplitude was 18.2±1.1 mV and the mean number of spikes evoked by the cEPSP was 3.4±0.2. The mean amplitude of cEPSPs in APRs with anterior cell bodies (19.7±1.5 mV; $N=12$) differed significantly from mean cEPSP amplitude in APRs with posterior cell bodies (16.6±1.4 mV; $N=12$; paired *t*-test, $P<0.05$). However, the mean number of spikes evoked per stimulus did not differ significantly for APRs with anterior and posterior cell bodies

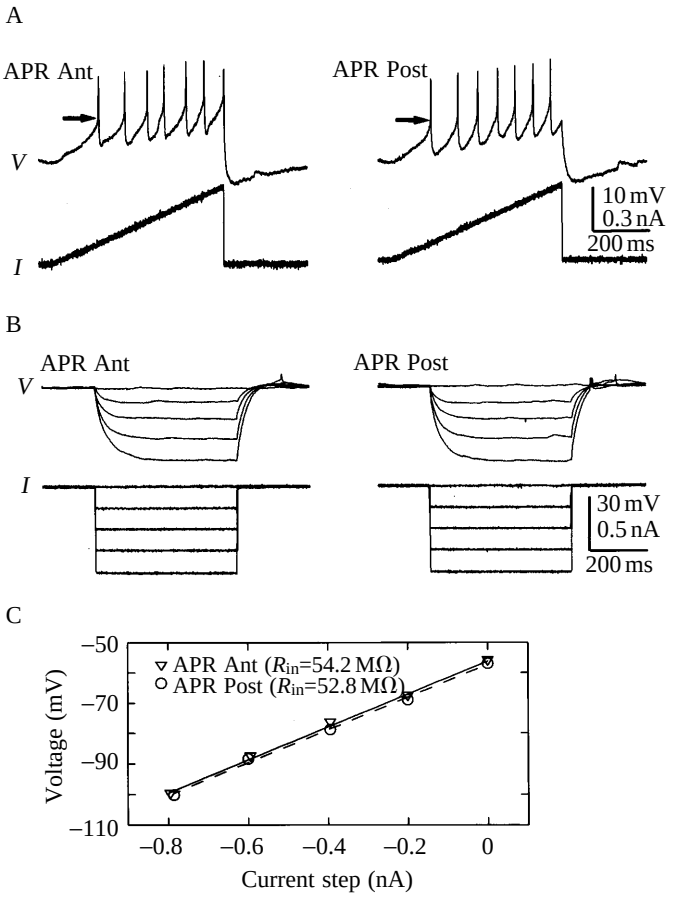

Fig. 2. Electrical properties of APRs. All recordings are from the same pair of APRs, designated by their anterior (Ant) or posterior (Post) soma position. (A) Spike threshold was measured by injecting a 500 ms ramp of depolarizing current (maximum value, 0.5 nA) into each APR from a starting potential of −60 mV (SEC mode). The spike thresholds (arrows) were −48.7 mV and −49.6 mV for the anterior and posterior APRs, respectively. Resting membrane potential (V_m) was −53.9 mV for the anterior APR and −55.5 mV for the posterior APR. (B) Current–voltage relationship. The APRs were held at −60 mV and current steps up to −0.8 nA were injected (bottom traces). The resulting voltage deflections (top traces) were similar in amplitude and time course. (C) Current–voltage plot of the experiment shown in B; triangles and circles are from the anterior and posterior APR, respectively. The slopes (input resistance, R_{in}) of the plots (values given in the figure) were nearly identical. *I*, current; *V*, voltage.

Table 1. *Electrical properties of proleg motoneurons*

	V_m (mV)	Threshold (mV)	R_{in} (MΩ)	τ_m (ms)
Accessory planta retractor motoneuron				
Anterior (N=10)[a]	–54.2±1.2	–44.0±0.8	49.5±4.2	27.4±2.4
Posterior (N=10)[a]	–53.0±0.8	–45.1±0.7	53.2±1.9	28.3±1.8
Total (N=27)[b]	–53.1±0.7	–44.1±0.5	51.8±1.9	27.9±1.1
Principal planta retractor motoneuron	–43.5±4.6[c]	–52.9±1.3[d]	12.7±3.3[e]	ND

Values are means ± S.E.M.

[a]Anterior and posterior members of each APR pair did not differ significantly in any parameter (paired *t*-test, P>0.25).

[b]10 pairs from above, plus seven APRs whose soma positions were not determined.

[c]Trimmer and Weeks (1989) (N=73).

[d]Trimmer and Weeks (1993) (N=5).

[e]Trimmer and Weeks (1989) (N=24).

ND, no data; V_m, membrane potential; R_{in}, input resistance; τ_m, membrane time constant.

(3.5±0.2 spikes for anterior cells and 3.4±0.3 spikes for posterior cells; paired *t*-test, P>0.3; N=12 pairs).

Although anterior APRs, as a group, had a larger mean cEPSP amplitude than did the group of posterior APRs, the preceding analysis did not indicate the proportion of instances in which cEPSP amplitude differed significantly between the two members of an APR pair. Therefore, in a second analysis, for every pair of APRs (N=12 pairs), we compared the responses of each member to individual VN_{AABr3} stimuli (4–8 trials per APR). In 8 of 12 pairs of APRs, the two APRs exhibited indistinguishable responses to VN_{AABr3} stimuli: mean cEPSP amplitude and the mean number of evoked spikes did not differ significantly (paired *t*-test, P>0.10). This response pattern is illustrated in Fig. 3Ai. In the remaining four pairs of APRs, three pairs differed significantly in cEPSP amplitude and number of evoked spikes (e.g. Fig. 3Aii), and one pair differed only in the number of evoked spikes (paired *t*-test, P<0.05); it was the anterior APR that responded more strongly in three of these four cases. The proportion of APR pairs that showed significantly different responses was similar when the APRs were recorded simultaneously (one of five pairs different) or sequentially (three of seven pairs different). In summary, all APRs were strongly excited by stimulation of PH sensory neurons, but anterior APRs tended to exhibit larger cEPSPs.

IN-703 produces apparently monosynaptic EPSPs in contralateral APRs located in the same ganglion (Sandstrom and Weeks, 1991*a*). During intracellular recordings from an IN-703, members of APR pairs were impaled sequentially and found to receive qualitatively similar EPSPs which occurred after a similar latency (Fig. 3B; N=4). EPSP amplitude in the second APR impaled (Fig. 3Bii) was always smaller than that recorded in the first APR impaled (Fig. 3Bi), irrespective of APR cell body position (data not shown): repetitive stimulation of IN-703 to obtain a signal-averaged EPSP in the first APR appeared to cause long-lasting depression of EPSP amplitude that persisted longer than the longest recording times (30–60 min). These recordings indicated that IN-703 produced qualitatively similar EPSPs in both APRs of a pair, although quantitative comparisons were not possible.

Synaptic inputs from PH sensory neurons and IN-703 presumably represented only a small sample of the total synaptic inputs to the APRs. To investigate synaptic inputs from other, unidentified sources, we recorded spontaneous synaptic potentials in pairs of APRs in whole nerve cords. These recordings showed a preponderance of common inputs to the APRs, although some synaptic events were observed in only one APR of a pair (Fig. 3Ci). For comparison, we recorded simultaneously from an APR and MN-1, which innervates a dorsal body wall muscle and whose dendritic arborization occupies the same general region of dorsal neuropil as that of the APRs (Levine and Truman, 1985). Recordings from an APR and MN-1 revealed few similar inputs and many dissimilarities (Fig. 3Cii). To compare quantitatively the spontaneous synaptic inputs to APR and MN-1, recordings were digitized, plotted on *x-y* coordinates and coefficients of correlation (*r*-values) were calculated. Because the correlation coefficients assessed the *direction* of change in membrane potential rather than the absolute amplitude of the change, differential damage to one or the other neuron or differences in electrotonic distance from synaptic sites to the soma were not confounding factors. Voltage fluctuations in APR pairs were strongly correlated (Fig. 3Di; mean *r*-value=0.80±0.02, N=7 pairs) whereas fluctuations in APR and MN-1 pairs were substantially less well correlated (Fig. 3Dii; mean *r*-value=0.27±0.09, N=6 pairs). In four of these preparations, simultaneous recordings were made from both an APR pair as well as from one of the APRs and MN-1 (the order of the impalements varied). The correlation coefficients of the APR pairs, and the APR and MN-1 pairs, differed significantly (paired *t*-test, P<0.001). Hence, spontaneous synaptic inputs to members of APR pairs were highly correlated and significantly less well correlated with inputs to MN-1.

Because similarity in the synaptic inputs of the APRs could have resulted from electrical coupling, we attempted to pass current between members of APR pairs. Currents between −5.0 and +5.0 nA injected into one APR produced no detectable voltage deflections in the other APR (data not shown; N=5). Furthermore, in hundreds of APRs injected with cobalt, and dozens stained with biocytin or Lucifer Yellow, dye was never observed to pass to another APR (data not shown). Therefore, ipsilateral pairs of APRs appeared not to be electrically or dye coupled.

Innervation of the APRM by the APRs

We next examined how the two APRs shared innervation of the APRM. The preparation shown in Fig. 4A permitted the APRs to be stimulated (by extracellular stimulation of VN_L or intracellular current injection; see Materials and methods)

while recording intracellularly from individual APRM fibers. APRM fibers were arranged in two layers, one external (adjacent to the body wall) and one internal. Individual fibers were often 'V'- or 'N'-shaped; these were counted as single fibers because current injected into one branch of the fiber readily passed into other branches (coupling coefficient >0.4; *N*=4). In some cases, fibers were electrically coupled without obvious cytoplasmic continuity (coupling coefficient <0.15; *N*=3). The mean number of fibers in APRMs from segments A3, A4 and A5 was 5.3±0.2 (range, 3–7 fibers; *N*=52 muscles). When pinned in the recording chamber, the mean length of the APRM was 3.9±0.1 mm (*N*=43 muscles).

Insect skeletal muscles, including those of larval Lepidoptera, typically exhibit both synaptic conductances and voltage-dependent conductances (e.g. Dietmer, 1977; Rheuben and Kammer, 1983; Bindokas and Adams, 1990; Singh and Wu, 1990). When APRMs were bathed in physiological saline that mimicked the composition of the hemolymph (containing a high $[K^+]$ and a low $[Na^+]$; Weeks and Truman, 1984*b*), APR stimulation evoked muscle potentials with obvious regenerative components (data not shown). Because we were interested in the properties of the underlying EJPs and not the active muscle currents, we instead bathed APRMs in the same saline used for desheathed ganglia (containing a high $[Na^+]$ and a low $[K^+]$; see Materials and methods), which eliminated most or all of the active muscle currents (see below). Under these conditions, the mean V_m of APRM fibers was −51.3±0.6 mV (*N*=108 fibers in 34 muscles) and the mean R_{in} was 48.9±4.1 kΩ (*N*=18 fibers in 7 muscles). Over the range tested (approximately −90 to −30 mV), *I/V* relationships were linear (data not shown). Mean λ was 2.23±0.4 mm (*N*=7), indicating that the fibers were approximately 2λ in electrotonic length. These values are within the range published for other insect muscles (Rheuben, 1972; reviewed in Bindokas and Adams, 1990).

Fig. 4B shows potentials recorded in a singly innervated APRM fiber (see below) held at several values of V_m by injected current. The potentials rose and fell rapidly, and at resting V_m typically terminated in a small after-hyperpolarization (Fig. 4B,C). Several observations suggested that these potentials were predominantly synaptic. First, the

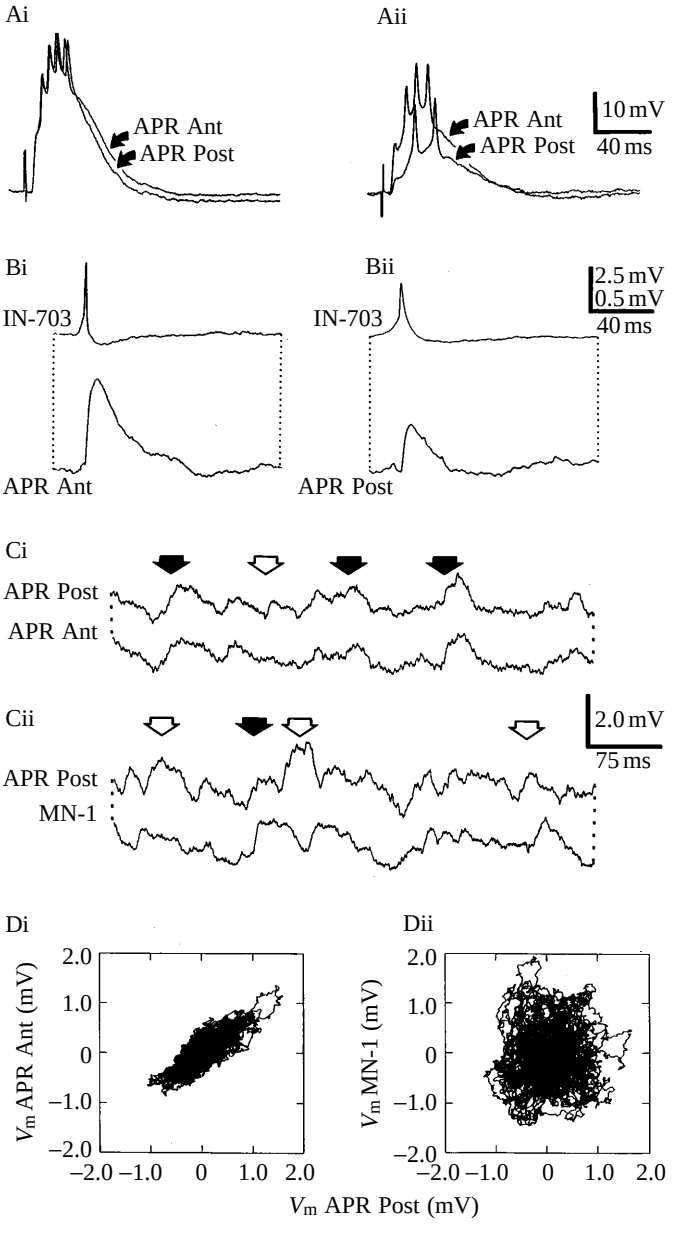

Fig. 3. Synaptic inputs to the APRs. (A) Input from planta hair (PH) sensory neurons. A pair of APRs was recorded simultaneously while the axons of the PH sensory neurons were stimulated electrically *via* single shocks to VN_{AABr3} (indicated by a vertical stimulus artifact). The APRs were held at −60 mV (SEC mode). In Ai, the stimulus evoked similar compound excitatory postsynaptic potentials (cEPSPs) and the same number of spikes in the two APRs. In a different pair of APRs (Aii), cEPSP amplitude and the number of evoked spikes differed between the two cells. (B) Input from IN-703 to a contralateral pair of APRs. The top traces show spikes in IN-703 while the bottom traces show the time-locked, unitary EPSPs in the anterior (Bi) and posterior (Bii) APRs. The APRs were recorded sequentially (anterior, then posterior), and the smaller amplitude of the EPSP produced by IN-703 in the posterior APR appeared to result from synaptic depression (see text). (C) Spontaneous synaptic inputs to APRs and MN-1. Ci shows spontaneous synaptic input to a pair of APRs, recorded simultaneously. Most inputs to the APRs were correlated (e.g. filled arrows), with occasional differences (open arrow). Cii shows spontaneous synaptic inputs to an APR and MN-1. After data had been sampled from the pair of APRs in Ci, the electrode was removed from the anterior APR and placed into the MN-1 whose cell body was contralateral to the APRs (and whose dendrites overlapped with those of the APRs). Some voltage fluctuations were common to the two neurons (filled arrow), but most were not (open arrows). (D) Comparison of spontaneous synaptic input to APRs and MN-1. In Di, 3.2 s of data from the experiment shown in Ci were digitized at 10 kHz and V_m of the posterior APR (*x*-axis) was plotted against that of the anterior APR (*y*-axis). Synchronous V_m fluctuations appear as positive correlations in the plot. These data were highly correlated (Pearson *r*-value = 0.81). Dii shows similar data for the APR and MN-1 in Cii. The correlation between voltage fluctuations in APR and MN-1 (*r*=0.04) was significantly lower than for the pair of APRs (*t*-test; *P*<0.0001).

rising phase of the potentials did not exhibit inflections indicative of voltage-dependent conductances (Cerf *et al.* 1959; Dietmer, 1977; Bindokas and Adams, 1990; Singh and Wu, 1990). Second, the amplitude of the potentials changed linearly with changes in V_m (Fig. 4B and data not shown), whereas voltage-dependent conductances should appear or disappear as V_m is varied (Cerf *et al.* 1959). Finally, the amplitude of the potentials declined gradually and continuously when APRs were stimulated at high frequencies (up to 200 Hz) and did not exhibit the abrupt loss of a regenerative component (data not shown; Cerf *et al.* 1959). Therefore, the rising phase of the APR-evoked potentials in APRM fibers appeared to be due to synaptic rather than to voltage-dependent currents. However, the presence of the small after-hyperpolarizations suggested that one or more outward currents (e.g. Singh and Wu, 1990) persisted. We henceforth refer to these APR-evoked potentials as EJPs.

By recording from multiple fibers in an APRM while stimulating the APRs, we determined that some fibers were singly innervated by one or the other APR (Fig. 4Ci,ii), while other fibers were dually innervated by both APRs (Fig. 4Ciii). The properties of EJPs in singly innervated fibers are described first, followed by those of dually innervated fibers. A pair of cells with neurosecretory morphology (cells 16 and 17 of Taylor and Truman, 1974) sometimes stain in cobalt backfills of VN_L (Weeks and Davidson, 1994), but no electrophysiological or anatomical evidence suggests that these cells innervate the APRM (see below, and data not shown). Likewise, intracellular recordings from APRM fibers did not provide any evidence of inhibitory innervation (N=150 fibers in 50 muscles). Therefore, the designations 'singly innervated' or 'dually innervated' refer to the innervation of APRM fibers by the APRs. The amplitude of EJPs (V_{EJP}) in singly innervated fibers was consistently large (mean value=31.2±0.6 mV) and time-to-peak (t_p) was short (mean value=5.8±0.1 ms; N=72 fibers in 32 muscles). These properties are similar to those reported for EJPs produced by fast excitatory motoneurons in insects (Hoyle, 1974; Hardie, 1976; Rheuben and Kammer, 1983; Sonea and Rheuben, 1992). For the subset of experiments in which APRs were impaled and their soma location determined, the amplitude and time-to-peak of EJPs produced by anterior APRs (N=12 fibers in 11 muscles) and posterior APRs (N=7 fibers in 6 muscles) in singly innervated fibers did not differ significantly (V_{EJP}=30.5±2.1 mV for anterior APRs and 30.1±9.5 mV for posterior APRs; t_p=6.5±0.3 ms for anterior APRs and 6.4±0.5 ms for posterior APRs; *t*-tests, P>0.5). The calculated E_{rev} for EJPs was −1.99±2.3 mV (N=6 fibers in 4 preparations), consistent with glutamate being the excitatory neurotransmitter (Pichon and Ashcroft, 1985). EJPs from all APRs showed similar decreases

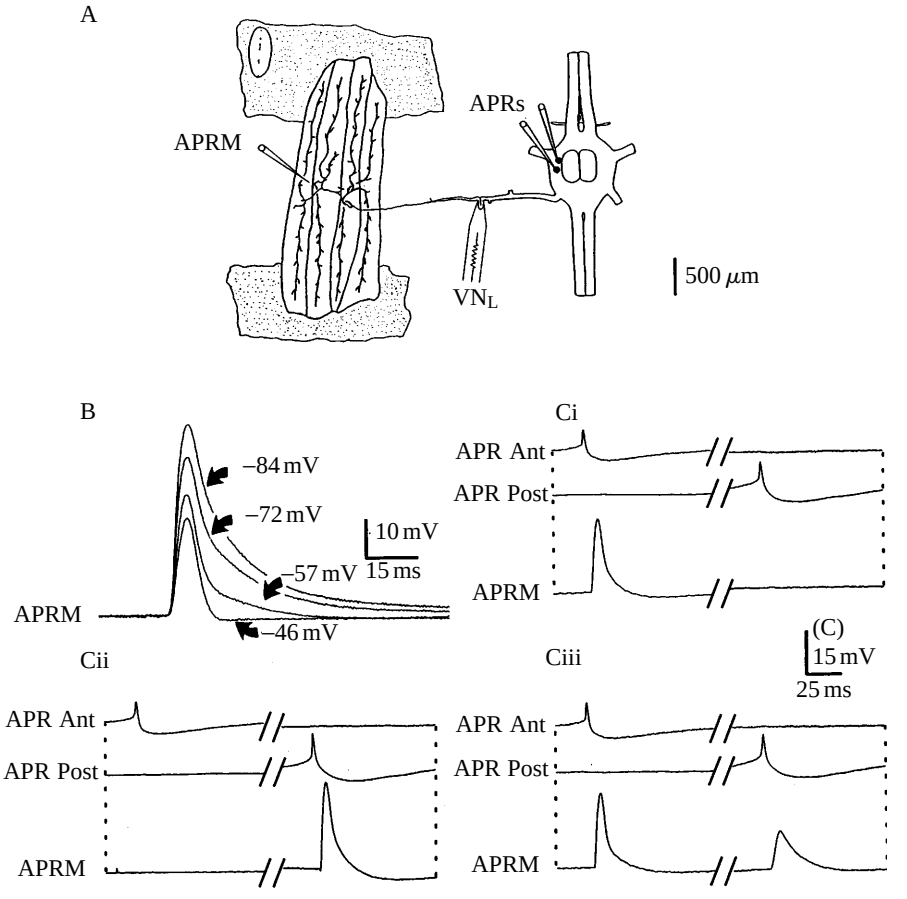

Fig. 4. Innervation of the APRM by the APRs. (A) The preparation consisted of the APRM from a right hemisegment (pinned by attached cuticle; stippled) and the ganglion from the same segment. The spiracle (oval at upper left) is also shown. APRs were stimulated either *via* extracellular shock of the lateral branch of the ventral nerve (VN_L, B) or by intracellular current injection (Ci–iii). Muscle potentials were recorded intracellularly. (B) Excitatory junction potentials (EJPs) evoked by an APR in a singly innervated fiber, which was held at V_m values between −46 and −84 mV. At all values of V_m, the EJP rose rapidly and monotonically: in this fiber, time-to-peak (t_p) was 4.4 ms and excitatory junction potential amplitude (V_{EJP}) was 28.4 mV at resting V_m (−57 mV). The EJP terminated in an after-hyperpolarization, which was most apparent at −46 mV. (C) Examples of single and double innervation of APRM fibers. All recordings are from the same preparation. In each panel, the top two traces are simultaneous intracellular recordings from the pair of APRs ipsilateral to the APRM, while the bottom trace is an intracellular recording from an APRM fiber (averages of three sweeps per data segment). Ci shows single innervation of an APRM fiber by the anterior APR, which produced an EJP in the fiber although the posterior APR did not. Cii shows single innervation of a different APRM fiber by the posterior APR. In Ciii, both the anterior and posterior APRs produced EJPs in a third fiber in the same muscle. As was typical for dually innervated fibers, the EJPs had dissimilar sizes and shapes.

in V_{EJP} with repetitive stimulation at frequencies above 0.03 Hz (data not shown).

An example of dual innervation is shown in Fig. 4Ciii: both the anterior and posterior members of an APR pair produced EJPs in an APRM fiber. However, the anterior APR produced a large, rapidly rising EJP while the posterior APR produced a small, broad EJP. The same posterior APR produced a large, rapidly rising EJP in a different, singly innervated fiber in the same muscle (Fig. 4Cii). A consistent pattern was that all EJPs in singly innervated fibers had a large V_{EJP} and a short t_p (see above), whereas the size and shape of EJPs in dually innervated fibers varied. One hypothesis to explain these differences was that, in singly innervated APRM fibers, the APR innervated the fiber uniformly along its length, whereas in dually innervated fibers, the two APRs innervated non-overlapping regions of the fiber. This hypothesis predicted that V_{EJP} should be large and t_p short at all sites on singly innervated fibers, whereas V_{EJP} and t_p should vary by recording site along dually innervated fibers. We tested this hypothesis by recording V_{EJP} and t_p at different sites along the dorsoventral length of singly and dually innervated APRM fibers.

In singly innervated APRM fibers, V_{EJP} and t_p (Fig. 5A) were uniform along the dorsoventral extent of the fiber (55 of 56 fibers, in 22 muscles). These findings are consistent with singly innervated fibers being innervated uniformly along their lengths by a single APR; anatomical data supporting this interpretation appear below.

In dually innervated APRM fibers, the EJPs from the two APRs were complementary (25 of 36 fibers, in 14 of 16 muscles): one APR produced EJPs that were largest at the ventral end of the fiber and became smaller towards the dorsal end of the fiber, while the other APR produced EJPs that were largest at the dorsal end and smallest at the ventral end (Fig. 5B). Because of the complementary effects of the two APRs, the muscle fiber was depolarized rapidly and uniformly when both APRs fired simultaneously (Fig. 5B). There was an inverse correlation between V_{EJP} and t_p, suggesting that the synaptic terminals of the two APRs were segregated in dorsal and ventral regions of the muscle and that the small, broad EJPs resulted from electrotonic decay from the site of the motor terminals (Jack *et al.* 1975). This conclusion is supported by anatomical data (see below).

One additional pattern of EJP properties was seen, associated with electrical coupling between muscle fibers (9 of 36 fibers, in 6 of 16 muscles). In these cases, one APR produced large, rapidly rising EJPs along the length of the fiber while the other APR produced a small, slow EJP at one end of the fiber (Fig. 5C). In other systems, this pattern has been attributed to electrical coupling between muscle fibers (e.g. Cohen *et al.* 1978). In one preparation, a small, slow EJP was recorded at the site of strongest electrical coupling between two APRM fibers, and the EJP decreased in size with distance from that site (data not shown): this finding is consistent with the small, slow EJPs being coupling potentials. The small amplitudes of these EJPs (Fig. 5C) made them unlikely to play

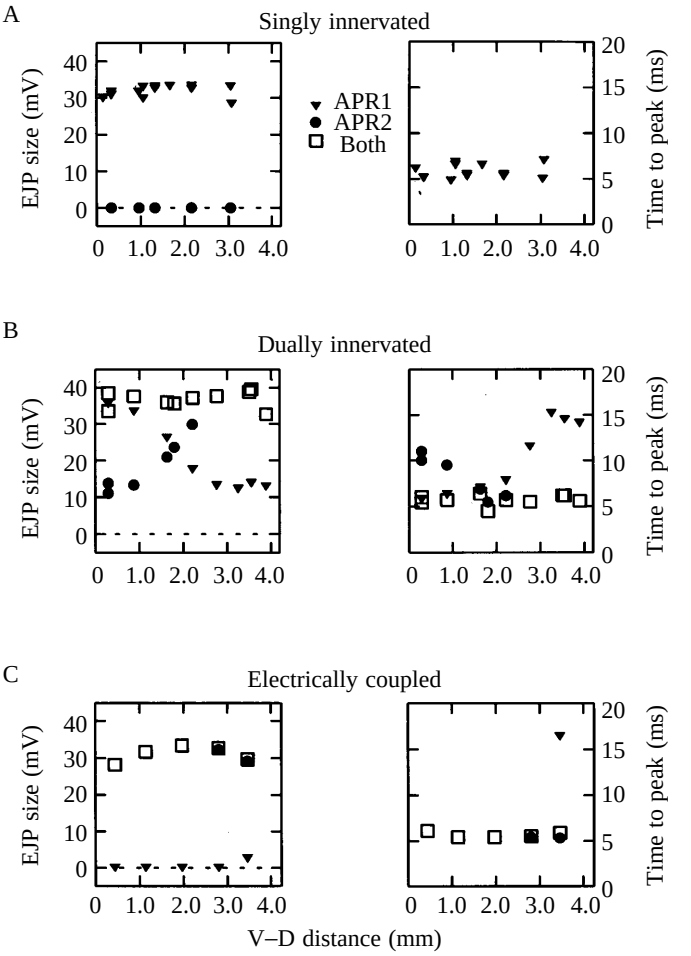

Fig. 5. Relationship between EJP properties and recording site in APRM fibers. In three different muscle fibers (A, B and C), V_{EJP} and t_p were measured at multiple sites along the length of the fiber from ventral to dorsal (V−D distance). The APRs were stimulated extracellularly *via* the VN_L, so their soma positions were not known, and they were arbitrarily designated 'APR1' and 'APR2'. The stimulation voltage applied to VN_L was adjusted to activate just APR1 (filled triangles), just APR2 (filled circles) or both APRs synchronously (open squares). During EJP recordings at some sites, only a subset of the three types of stimulation was tested. In the V_{EJP} plots (at left), a dashed line indicates 0 mV (undetectable voltage response in the muscle fiber). (A) This singly innervated fiber was innervated only by APR1. V_{EJP} and t_p were relatively uniform throughout its length. (B) In this dually innervated fiber from a different preparation, both APRs innervated the fiber, but their V_{EJP} and t_p varied in a graded fashion along the length of the fiber. V_{EJP} and t_p for the two APRs were complementary, such that V_{EJP} and t_p were relatively uniform throughout the fiber when both APRs fired simultaneously. (C) In a fiber from a different preparation, one APR produced large EJPs while the other APR produced a very small EJP at one end. EJPs were produced exclusively by APR2 at sites 0–3 mm from the ventral end of the fiber (because stimulation of APR1 produced no effects there), but the EJPs are shown as open squares because APR2 could not be stimulated alone during recordings from those sites. t_p was short for EJPs from the dominant APR and long for EJPs from the other APR. Fibers with these properties were scored as being singly innervated (in this case, by APR2), with the small EJPs arising from electrical coupling to another APRM fiber innervated by the other APR (in this case, APR1).

a significant functional role, so they were disregarded when scoring fibers as singly or dually innervated.

In the remaining fibers (two fibers in two different muscles), EJP properties did not follow a clear spatial pattern so were not analyzed further.

In preparations in which EJP properties were mapped for all fibers in an APRM (N=12), the results were projected onto drawings of the muscles (Fig. 6A–C). In dually innervated fibers, we assumed that the regions in which V_{EJP} amplitudes were maximal represented the regions innervated by each APR. Fig. 6A shows an APRM that contained exclusively singly innervated fibers, whereas Fig. 6B and Fig. 6C show APRMs with a mixture of singly and dually innervated fibers. The mean percentage of dually innervated fibers in APRMs was 33 % (range, 0–100 %; N=12), and 75 % of the APRMs (9/12) had at least one dually innervated fiber. The arrangement of APR innervation fields within APRM varied. In 5 of 12 APRMs, the regions innervated by the two APRs were clearly divisible into anterior and posterior domains (e.g. Fig. 6A,B). Soma positions of the APRs were not correlated with their region of innervation (data not shown). In the remaining APRMs (7 of 12), both APRs innervated fibers scattered throughout the muscle (e.g. Fig. 6C). This pattern correlated with a higher proportion of dual innervation.

Anatomy of APR motor terminals

To examine whether the anatomical arrangement of APR terminals on APRM fibers was consistent with the inferred innervation fields based on EJP measurements (Figs 5, 6A–C), we stained APR motor terminals with cobalt. Anterograde cobalt staining of both APRs *via* the VN revealed terminals of approximately uniform morphology along the lengths of all APRM fibers, except at their extreme dorsal ends (Fig. 6D; N=21 muscles). This finding supported the conclusion from electrophysiological studies (Fig. 5) that APRM fibers were uniformly innervated along their lengths. When individual APRs were stained by intracellular cobalt injection (N=4), the extent of their terminal fields varied (Fig. 6E,F). Some APRM fibers were innervated by the terminals of the stained APR along their entire lengths (Fig. 6E,F), representing single innervation. Other fibers were innervated by the stained APR for only a portion of their lengths (Fig. 6F); presumably, the region of the fiber lacking stained terminals was innervated by the other APR, representing dual innervation. The anatomical

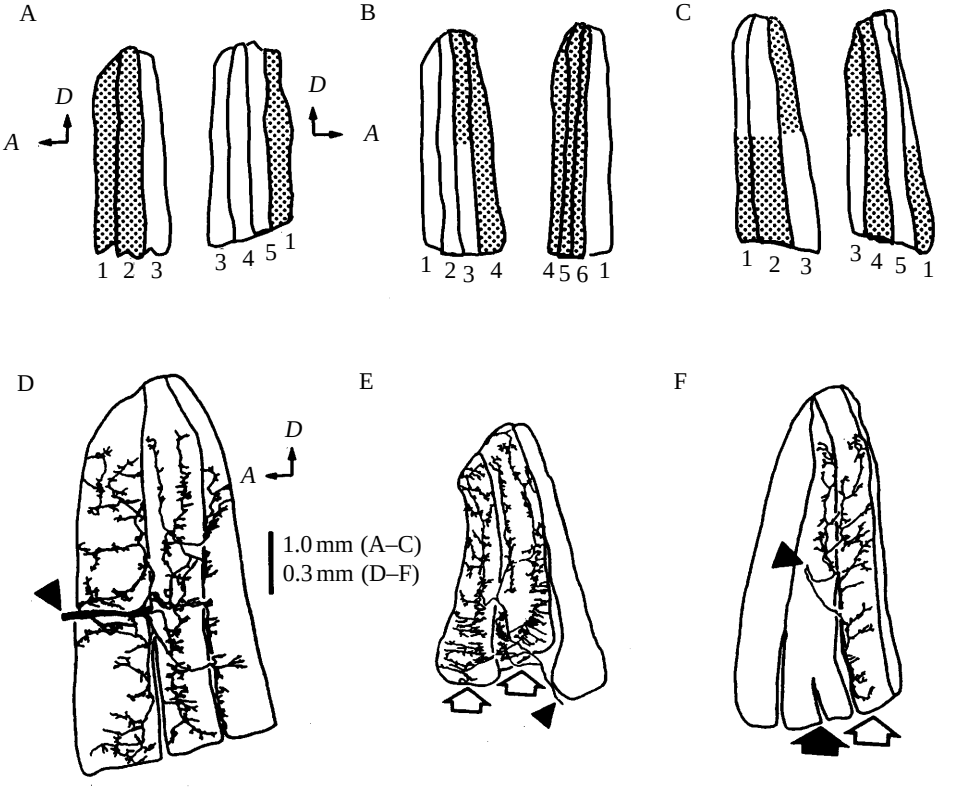

Fig. 6. Innervation patterns of APRMs. (A–C) The regions inferred to be innervated by the two APRs are displayed on *camera lucida* drawings of three different APRMs whose EJPs were mapped completely (as in Fig. 5). None of the fibers exhibited EJPs from electrical coupling with other fibers. In each panel, the internal (left) and external (right) surfaces of the muscle were drawn. Fibers were assigned numbers from left to right, starting on the internal surface; some fibers were visible from both internal and external surfaces (e.g. A, fibers 1 and 3) while others were visible from only one surface (e.g. A, fibers 4 and 5). Arrows indicate dorsal (*D*) and anterior (*A*). Regions innervated by one APR are stippled and those innervated by the other APR are unshaded. (A) The APRs innervating this APRM split the muscle into anterior and posterior domains. No dually innervated fibers were present. (B) This APRM was also innervated in anterior and posterior domains and had one dually innervated fiber at the intersection of the two domains. (C) In this APRM, three of five fibers were dually innervated. The domains of the two APRs were scattered throughout the muscle. (D–F) Anatomical arrangement of APR terminals on APRM. The internal surface of each muscle is shown, with the incoming nerve indicated by an arrowhead. The muscles are smaller than in A–C because they were taken from younger larvae (see Materials and methods). (D) Both APRs were stained anterogradely *via* the VN. All three fibers shown were innervated along their lengths except for the far dorsal ends. (E) A single APR was stained by intracellular cobalt injection. Two fibers were innervated along their lengths (open arrows) while a third fiber had no stained terminals. (F) The terminals of another APR, stained as in E. This APR innervated one fiber along its length (open arrow) and the dorsal half of another fiber (filled arrow). The third fiber shown had no stained terminals.

patterns of APRM innervation thus matched the innervation patterns inferred from EJP measurements (Fig. 6A–C).

Activity of APRs during the proleg withdrawal reflex

The similarities between members of APR pairs suggested that they might exhibit similar activity during proleg behaviors, such as the withdrawal reflex (Weeks and Jacobs, 1987). Using the semi-intact preparation shown in Fig. 7A, we deflected individual PH hairs while monitoring activity in the ipsilateral pair of APRs by recording their EJPs in APRM fibers (N=11 preparations). Activity in the two APRs was discriminated by recording from two singly innervated APRM fibers or, in some cases, from regions of dually innervated fibers where the two APRs produced EJPs of clearly different amplitudes (e.g. Fig. 7C). Each EJP indicated a spike in the respective APR. In each preparation, we briefly deflected a single PH in the middle, distal region of the PH array (Peterson and Weeks, 1988) for 20 trials. The interval between trials varied but was always greater than 30 s. The two APRs were then impaled to determine their soma positions and one APR was stained intracellularly with cobalt.

Fig. 7B shows the EJPs produced by one pair of APRs during four representative PH deflections. The APRs were silent until PH deflection, which evoked a bout of activity. The pattern of EJPs evoked by PH deflection had two components. First, there was an initial cluster of EJPs which occurred reliably each time a PH was deflected. After this period, the EJPs either ceased (e.g. Fig. 7B, trial 5) or continued at lower frequency (e.g. Fig. 7B, trial 9). In a few preparations, the second component of the response consisted of continued activity for several minutes (data not shown). We counted the number of EJPs produced by each APR during the first 500 ms (to include the first component of the response) and during the total response to each stimulus (to include both components).

For all APRs tested, the mean number of EJPs produced per trial was 2.3±0.2 for the first 500 ms of the response and 8.2±2.5 for the total response (N=22 APRs in 11 ganglia, each with 20 trials). When data from anterior and posterior APRs were compared (N=11 APRs per group), the number of EJPs produced in the first 500 ms differed significantly, with anterior APRs producing the stronger response (anterior APRs, 2.6±0.3 EJPs; posterior APRs, 2.1±0.4 EJPs; paired t-test, P<0.025). However, the number of EJPs produced during the total response did not differ significantly between anterior and

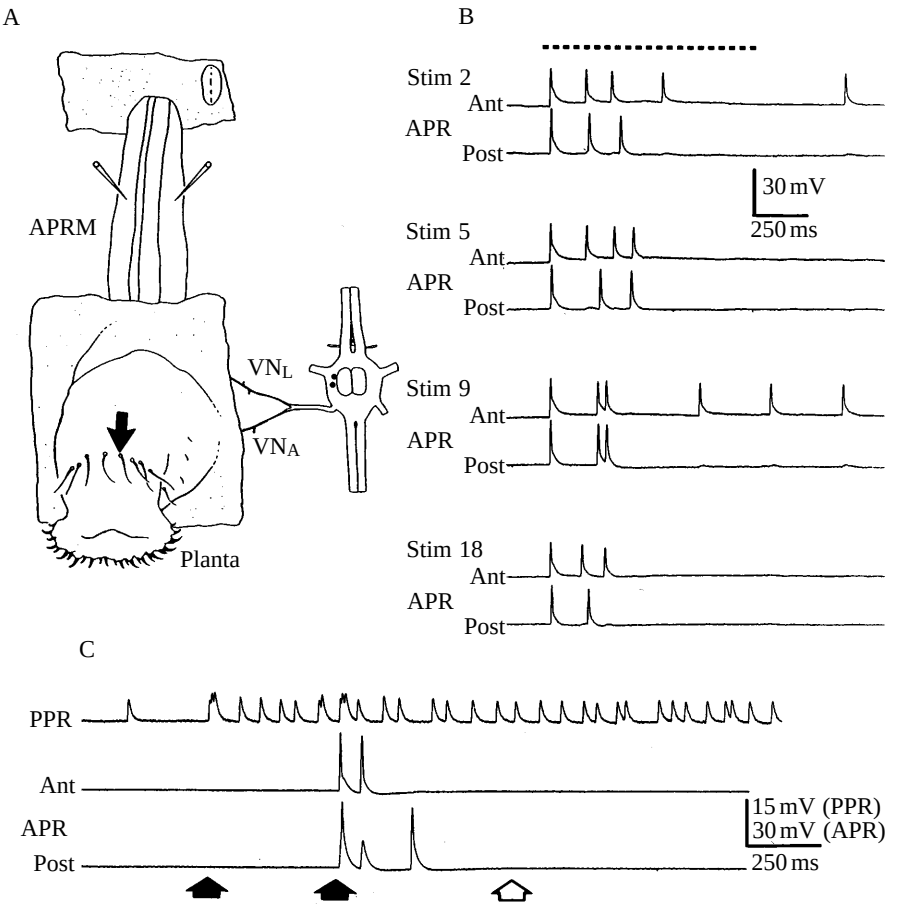

Fig. 7. Activity of the APRs during PH deflection. (A) The preparation consisted of an isolated proleg, its associated ganglion and the APRM. One middle PH (arrow; only the distalmost row of PHs is drawn) was briefly deflected in the dorsal (most sensitive) direction. Intracellular recordings were made from muscle fibers to record EJPs evoked by PH deflection, and the cell body positions of the APRs were determined at the end of the experiment by intracellular impalements. The intracellular recordings from muscle fibers shown in B and C are labeled by the identity of the motoneuron that innervated the fiber. VN$_L$, VN$_A$, lateral and anterior branches of the ventral nerve. (B) Four representative responses to PH deflection (from a total of 20 trials) in one preparation. The dashed line above the top trace indicates the approximate duration of the PH deflection in each trial. Each trace shows all EJPs evoked by the stimulus (Stim). Responses consisted of an initial cluster of EJPs followed by a period of silence or low activity. The anterior APR consistently responded more strongly to PH deflection than did the posterior APR. (C) Responses of the principal planta retractor motoneuron (PPR) and the APRs to PH deflection. In this preparation, PPRM and APRM were left attached to the proleg. In the APRM recordings, the upper trace shows a fiber singly innervated by the anterior APR while the lower trace shows a dually innervated fiber in which the posterior APR produced large EJPs and the anterior APR produced small EJPs. A PH was deflected partially (first filled arrow) and held in that position, and then deflected more fully (second filled arrow). The open arrow shows the approximate time when the PH was released. PPR responded more strongly than the APRs (see text).

posterior APRs (anterior APRs, 9.4±4.6 EJPs; posterior APRs, 7.1±2.4 EJPs; paired *t*-test, $P>0.05$).

We also compared how the two APRs in each pair responded to each PH deflection during the series of 20 trials. In 8 of the 11 pairs, the number of EJPs produced by the two APRs during the first 500 ms differed significantly (paired *t*-test, $P<0.05$; $N=20$ trials), and in seven of these eight cases the anterior APR showed the stronger response. Similarly, the number of EJPs produced by each APR during the total response differed significantly in 7 of 11 pairs (paired *t*-tests, $P<0.05$; $N=20$ trials), and in every case the anterior APR was the more responsive. Among APR pairs that differed in the number of EJPs evoked by PH deflection, anterior APRs were significantly more likely to produce the stronger response than expected by chance (seven of eight anterior APRs for the first 500 ms, seven of seven anterior APRs for the entire response; chi-square test, $P<0.05$). The same seven anterior APRs produced a significantly greater number of EJPs during both the first 500 ms and the total response. These findings are consistent with the finding presented above that anterior APRs tended to be more strongly excited by VN_{AABr3} stimulation (which activates PH sensory neurons) than are posterior APRs. The location of the medially directed neurite of an APR (Fig. 1D) was not correlated with the intensity of its response to PH deflection (data not shown).

Finally, we recorded from PPRM as well as APRM ($N=2$ preparations) to compare APR and PPR responses to PH deflection. Spontaneous EJPs were typically present in PPRM, indicating spontaneous firing in PPR. Fig. 7C illustrates the responses of PPR and the APRs to PH deflection. At the first filled arrow, a PH was partially deflected and held in this position, causing an increased rate of EJPs in PPRM but no response in APRM. At the second filled arrow, the PH was deflected more fully, again increasing EJP rate in PPR and evoking a brief response in the two APRs. The number of EJPs produced by PPR and the two APRs was measured for the first 500 ms following each PH deflection ($N=20$ PH deflections per preparation). PPR produced significantly more EJPs than did either APR in both preparations (paired *t*-tests, $P<0.001$). For example, for the preparation shown in Fig. 7C, the mean number of EJPs produced in the first 500 ms following PH deflection was 10.5±0.7 for PPR, 2.8±0.4 for the anterior APR and 2.0±0.4 for the posterior APR ($N=20$ trials). The finding that PPR was spontaneously active and more strongly excited by PH deflection than were the APRs was consistent with the observed differences in the electrical properties of the motoneurons (Table 1; see Discussion).

Discussion

Similarities and differences between members of APR pairs

Morphology

The only obvious structural variation among APRs was in the location of a large, medially directed neurite, which was sometimes dorsal and sometimes intermediate in the neuropil (Fig. 1D). The position of this neurite was observed in all possible combinations in members of APR pairs. Dorsal and intermediate neurites were equally common in APRs with anterior somata, whereas posterior APRs exhibited a higher proportion of dorsal neurites than expected by chance. Variability in the morphology of identified neurons is common, even among isogenic animals (e.g. Steeves and Pearson, 1983). The functional significance of APR neurite position, if any, is unknown: most synaptic inputs to the APRs presumably occur on the higher-order branches (e.g. Watson *et al.* 1985), which occupied similar neuropil regions in all APRs (Fig. 1C,D), and differences in the intensity of the responses of APRs to PH deflections were unrelated to neurite position.

Electrical properties and synaptic inputs

The intrinsic electrical properties of members of APR pairs were indistinguishable (Fig. 2; Table 1). This similarity implied a functional uniformity, particularly when compared with other identified *M. sexta* motoneurons, which exhibit different cell-specific electrical properties (e.g. PPR, Table 1; intersegmental muscle motoneurons, Waldrop and Levine, 1989). Tests for electrical coupling between members of APR pairs were negative, as is typical for insect motoneurons (discussed in Siegler, 1982).

Members of APR pairs exhibited qualitatively similar responses to all synaptic inputs examined. In most cases, the responses were quantitatively similar as well. Electrical stimulation of the proleg sensory nerve, to activate all of the PH sensory neurons simultaneously, evoked large cEPSPs and action potentials in both members of APR pairs, and in the majority (75 %) of cases the responses of the two APRs did not differ significantly (Fig. 3A). Spontaneous synaptic inputs to APR pairs in isolated nerve cords were strongly correlated (Fig. 3Ci,Di), whereas spontaneous synaptic inputs to APRs and MN-1 were not (Fig. 3Cii,Dii). The latter finding suggested that the strong correlation in synaptic inputs to APRs reflected a functional similarity rather than being a nonspecific indicator of spontaneous activity in isolated nerve cords. Correlation in the synaptic inputs of the APRs suggested that many presynaptic neurons made parallel connections with both members of APR pairs. Indeed, at least one identified interneuron, IN-703, synapses on both APRs (Fig. 3B). These observations on APR pairs are consistent with other reports of functionally synergistic neurons that receive parallel inputs from the same presynaptic sources (e.g. Mendell and Henneman, 1971; Burrows, 1975; Ferguson and Benjamin, 1991). Robertson (1990) described findings similar to ours for a pair of motoneurons that innervate separate regions of a locust flight muscle.

Although members of APR pairs exhibited many similarities, there were also small but consistent differences related to sensory input from PHs. Some APR pairs (25 %) differed significantly in the amplitude of the cEPSP and/or number of spikes evoked by electrical stimulation of the proleg sensory nerve (Fig. 3Aii). Furthermore, the majority (73 %) of APR pairs differed significantly in the number of spikes evoked by PH deflection (Fig. 7B). For both electrical and

mechanical stimulation of PH sensory neurons, anterior APRs were nearly always more strongly excited than were posterior APRs; for example, the anterior APR showed a significantly larger response to PH deflections in 88 % of pairs for the first 500 ms of the response and in 100 % of pairs for the total response. The different magnitudes of the responses of the APRs were not attributable to their intrinsic electrical properties (Fig. 2; Table 1), but instead could result from differences in the strength of mono- and/or polysynaptic connections from PH sensory neurons. For example, it was possible that PHs in the middle region of the PH array (which were stimulated in these experiments) excited anterior APRs more strongly than posterior APRs; the amplitude of monosynaptic EPSPs evoked in proleg motoneurons does vary by PH position (Weeks and Jacobs, 1987; Streichert and Weeks, 1995). However, in preliminary experiments, we deflected PHs in different locations on the proleg and found that the same APR was more responsive regardless of PH location (data not shown). Thus, the mechanism(s) underlying differential excitation of anterior and posterior APRs by PH sensory input remains unexplained. The functional consequences of preferentially activating one or the other APR is likewise enigmatic (see below).

Comparisons between APRs and PPR

The similarities between members of APR pairs are underscored when compared with the properties of PPR (Table 1; Fig. 7C). APRs were silent at rest, whereas PPR was tonically active. PH deflection more readily activated PPR than the APRs and the response of PPR was more prolonged than that of the APRs (Fig. 7B,C). These differences are predicted by differences in the electrical properties of the two types of motoneuron. Resting V_m of the APRs was approximately 9 mV more negative than spike threshold (Table 1) so that, in the absence of stimulation, the APRs are silent. In contrast, the V_m of PPR was approximately 9 mV more positive than its spike threshold (Table 1), causing spontaneous firing. These properties appear to have functional significance because, in intact larvae, weak PH stimulation causes only the planta to retract (as a result of PPRM contraction), whereas stronger PH stimulation is required to evoke retraction of the entire proleg (as a result of contraction of the APRM and other muscles; Weeks and Jacobs, 1987). PPRM contraction disengages the crochets on the planta from the substratum (Hinton, 1955), so recruiting PPR before the APRs ensures that the proleg is free to withdraw when the APRM contracts.

Dual innervation of the APRM by the APRs

As discussed in the following section, three features of the innervation of APRM by the APRs are noteworthy. First, innervation of an insect muscle by more than one functionally similar motoneuron is unusual. Second, the apparent segregation of the terminals of APRs on dually innervated APRM fibers appears to be unique, having some characteristics more typical of vertebrate neuromuscular junctions. Third, the variation in innervation patterns between preparations and the lack of overlap of the terminals of the APRs on the APRM suggest that the larval innervation pattern may be determined by a competitive mechanism.

Insect motoneurons have been divided into four functional categories (reviewed in Hoyle, 1974; Aidley, 1985): (1) fast excitatory motoneurons, which generate large, rapid EJPs that decrement upon repeated stimulation and produce phasic contractions; (2) slow excitatory motoneurons, which produce smaller, slower EJPs that facilitate upon repeated stimulation and produce smaller, slower contractions; (3) inhibitory motoneurons, which produce inhibitory junction potentials and muscle relaxation; and (4) modulatory neurons, which alter muscle excitability and/or contractility. The synaptic effects of the APRs on APRM fibers (Fig. 4) were characteristic of fast excitation. Although not tested directly, it is likely that the APRs release glutamate, the usual excitatory neuromuscular neurotransmitter in arthropods (Pichon and Ashcroft, 1985). Some insect motoneurons additionally release neuromodulators (e.g. Adams and O'Shea, 1983), but the APRs do not show immunoreactivity for octopamine (Pflüger *et al.* 1993), proctolin (Davis *et al.* 1989) or crustacean cardioactive peptide (Davis *et al.* 1993).

Multiple innervation of insect muscle fibers by combinations of the four neuronal types listed above is well described in the literature: singly innervated fibers are contacted by a single excitatory motoneuron whereas multiply innervated fibers are contacted by motoneurons with dissimilar synaptic effects (e.g. fast and slow excitation, or excitation and inhibition; Hoyle, 1955, 1974; Aidley, 1985). However, to our knowledge, multiple innervation of individual insect muscle fibers by motoneurons with a similar synaptic effect (e.g. fast excitation) has not been previously reported. Although there are examples of insect muscles innervated by more than one fast excitatory motoneuron (e.g. Kutsch and Usherwood, 1970; Kutsch and Schneider, 1987; Sonea and Rheuben, 1992), in these cases the motoneurons innervate non-overlapping subsets of fibers within the muscle. Thus, the APR/APRM neuromuscular system represents a novel form of multiple innervation in insects.

The segregation of the terminals of the APRs on APRM fibers is likewise unusual and shares some characteristics with multiply innervated vertebrate muscle. Two lines of evidence suggested that the terminals of the two APRs on dually innervated fibers were spatially segregated. First, t_p increased with decreasing V_{EJP} (Fig. 5B), consistent with electrotonic decay between the terminals of the APRs and the recording electrode (Jack *et al.* 1975). Second, cobalt-stained terminals of individual APRs covered some APRM fibers along their entire lengths and other fibers along only a portion of their lengths (Fig. 6E,F). This manner of innervation has not been reported previously. Among multiply innervated muscles in insects, motor terminals of the different motoneurons typically overlap and are not spatially segregated (reviewed in Hoyle, 1974; Keshishian *et al.* 1993). Although multiple innervation of single vertebrate muscle fibers is greatly reduced during embryonic and early postembryonic development (reviewed in

Colman and Lichtman, 1993), some of the exceptions show segregation of motoneuron terminals reminiscent of the innervation of the APRM. For example, in rat soleus muscle fibers that receive foreign innervation experimentally, multiple innervation is more stable when the terminals of the motoneurons are distant from one another (Kuffler *et al.* 1977). Factors that act to maintain separation of terminals innervating the same fibers in the frog pectoralis muscle have also been suggested (Nudell and Grinnell, 1983). Hence, the innervation of the APRM has characteristics of both insect and vertebrate neuromuscular junctions: the APR terminals are distributed along the fibers, which is typical of insects and unlike the circumscribed motor endplates of vertebrates, but the terminal fields of the two APRs are segregated from one another, which is previously unreported in insects but is seen in some multiply innervated vertebrate muscle fibers.

The segregation of the synaptic terminals of the APRs on the APRM and the variability of innervation patterns suggest that interactions between the two motoneurons and/or APRM determine the final distribution of the terminals. One possibility is that the variable innervation fields result from competition between the two functionally similar APRs for synaptic space on the muscle fibers. Competition among presynaptic neurons for postsynaptic sites is well-described for vertebrate synapses, including the neuromuscular junction (e.g. Colman and Lichtman, 1993). Competition similarly occurs at some arthropod synapses (reviewed in Lnenicka and Murphey, 1989), and insect motoneurons can exhibit considerable developmental plasticity in establishing innervation fields (Budnik *et al.* 1990; Keshishian *et al.* 1993). The embryonic development of the APRM neuromuscular junction could be a useful system for examining how axon terminals establish spatially segregated fields of innervation.

Possible functional role of dual innervation

The functional significance of the dual innervation of APRM remains unresolved. There was considerable variability in the number of APRM fibers innervated by a given APR, the proportion of those fibers that were singly or dually innervated, and the location of those fibers within the APRM (Fig. 6). There was no relationship between the soma position of an APR (anterior or posterior) and its pattern of innervation of the APRM. As discussed above, anterior APRs were usually more strongly excited by PH stimulation than were posterior APRs. However, given the variability with which members of APR pairs apportioned their innervation of the APRM, it is difficult to imagine how selective or stronger activation of one APR of a pair would have a significant behavioral effect. Activation of a single APR should produce a weaker proleg retraction than simultaneous activation of both APRs, an effect accomplished in singly innervated muscles by altering the firing rate of the motoneuron. Furthermore, although one APR may produce a slightly greater number of spikes in response to a given input (Figs 3Aii, 7), no stimuli have been found to activate only a single APR. It is possible, therefore, that the dual innervation of the APRM may have no functional consequence and results from evolutionary history rather than biological adaptation (see below). Although such a hypothesis is not readily testable, it is not unreasonable (Arbas *et al.* 1991; Kutsch and Breidbach, 1994).

Possible origins of dual innervation of the APRM by the APRs

Interestingly, the dual innervation of the APRM by a pair of APRs may be widespread among the Lepidoptera. Muscles similar to the APRM have been found in Bombycidae, Pyralidae, Pieridae and Saturniidae, and the presence of a pair of motoneurons with ventral somata and axons in the VN_L (i.e. potential APR homologs) has been observed in Bombycidae, Pyralidae, Saturniidae and Papilionidae (discussed in Sandstrom, 1993). In the silkworm *Bombyx mori*, the ventral motoneurons innervate the APRM-like muscle in a manner similar to that in *M. sexta* (data not shown). The finding of possible homologs of the APR/APRM neuromuscular system in divergent lepidopteran families suggests that components of this system may have been present for considerable evolutionary time.

How the dual innervation pattern arose during evolution is not known, but two hypotheses are tenable. One possibility is that the APRs originally innervated separate muscles and that the muscles either fused or one was lost. The developmental rearrangement and death of muscle precursors has been reported in insects (Ball *et al.* 1985), and insect motoneurons will innervate alternative targets when their normal targets are removed (Whitington, 1985; reviewed in Keshishian *et al.* 1993). The other possibility is that the two APRs arose from the duplication of a single APR, similar to the duplication or loss of neurons observed in other experimental systems (e.g. Doe *et al.* 1988; Mitani *et al.* 1993). Duplicated or supernumerary neurons have been reported in invertebrates (Kuffler and Muller, 1974; Treistman and Schwartz, 1976; Treistman, 1979; Dagan and Adams, 1981; Siegler, 1982), but the extra neurons are present only occasionally and their origin (*via* mutation or epigenetic events) is unknown. It would be instructive to know whether the two ventral motoneurons in distantly related families, such as the Pyralidae and the Papilionidae, innervate a single muscle as they do in *M. sexta* and *B. mori*.

Relevance to other studies of the APR/APRM system

The present study showed that the two members of APR pairs are indistinguishable by most criteria. This finding is consistent with other studies of the APRs' behavioral roles, synaptic connectivity, hormonal responses and metamorphic transformations, in which members of APRs pairs were assumed to be equivalent and in fact behaved uniformly (e.g. Weeks and Ernst-Utzschneider, 1989; Sandstrom and Weeks, 1991*a*; Weeks *et al.* 1992, 1993; Streichert and Weeks, 1994, 1995; Weeks and Davidson, 1994). There remain the unexplained findings that anterior APRs tend to be more strongly excited by PH sensory input than posterior APRs and that posterior APRs are biased towards having a dorsal neurite.

The only other instances in which members of APR pairs have been observed to behave dissimilarly occurred after experimental manipulations during the prepupal period, when APRs become committed to undergo programmed death; under these circumstances, one APR of a pair sometimes dies while its partner does not (Weeks *et al.* 1992, 1993; Weeks and Davidson, 1994). This dissociation appears to be probabilistic.

Although the two larval APRs that share innervation of each APRM are quite similar, two interesting *segmental* differences are manifested during metamorphosis. First, the death of APRs after pupation is segment-specific, with APRs in segments A2, A3 and A4 surviving while those in A1, A5 and A6 die (Weeks and Ernst-Utzschneider, 1989). Motoneuron death at pupation is controlled hormonally, by ecdysteroids (reviewed in Weeks *et al.* 1996), and the segment-specific pattern of APR death is expressed even when individual APRs are removed from the central nervous system, placed in culture and exposed to ecdysteroids (Streichert and Weeks, 1994; L. C. Streichert, J. T. Pierce and J. C. Weeks, unpublished observations). Thus, cellular interactions are not required for the correct pattern of APR death. A second segmental difference among APRs is that the threshold for initiating the death program in response to ecdysteroids is lower for APRs in A6 than for APRs in A5, which may explain the finding that APRs in A6 die earlier than APRs in A5 during normal development (Weeks *et al.* 1992). These observations indicate that a pattern of segment-specific attributes is superimposed on the otherwise similar properties of all APRs.

This research was supported by an NSF predoctoral fellowship and NIH predoctoral training grant support to D.J.S., and NIH grant R01 NS23208, NIH Career Development Award K04 NS01473, and an NSF Presidential Young Investigator Award to J.C.W. The authors thank Seana K. Davidson for assistance with histology, Julie Nelson for technical support and Charles Hedgcock, R.B.P., for photographic assistance. Drs E. A. Arbas, R. B. Levine, J. L. Lubischer, A. Novicki, W. M. Roberts, L. C. Streichert and E. R. Wood provided useful comments on the manuscript.

References

ADAMS, M. E. AND O'SHEA, M. (1983). Peptide cotransmitter at a neuromuscular junction. *Science* **221**, 286–289.

AIDLEY, D. J. (1985). Muscular contraction. In *Comprehensive Insect Physiology, Biochemistry and Pharmacology*, vol. 5 (ed. G. A. Kerkut and L. I. Gilbert), pp. 407–437. New York: Pergamon Press.

ARBAS, E. A., MEINERTZHAGEN, I. A. AND SHAW, S. R. (1991). Evolution in nervous systems. *A. Rev. Neurosci.* **14**, 9–38.

BALL, E. E., HO, R. K. AND GOODMAN, C. S. (1985). Muscle development in the grasshopper embryo. I. Muscles, nerves and apodemes in the metathoracic leg. *Dev. Biol.* **111**, 383–398.

BELL, R. A. AND JOACHIM, F. A. (1978). Techniques for rearing laboratory colonies of tobacco hornworms and pink bollworms. *Ann. ent. Soc. Am.* **69**, 365–373.

BINDOKAS, V. P. AND ADAMS, M. E. (1990). Neuromuscular transmission in larval tobacco budworm, *Heliothis virescens* (F.) (Lepidoptera: Noctuidae). *J. Insect Physiol.* **36**, 323–333.

BUDNIK, V., ZHONG, Y. AND WU, C. F. (1990). Morphological plasticity of motor axons in *Drosophila* mutants with altered excitability. *J. Neurosci.* **10**, 3754–3768.

BURROWS, M. (1975). Co-ordinating interneurones of the locust which convey two patterns of motor commands: their connexions with ventilatory motoneurones. *J. exp. Biol.* **63**, 735–753.

BURROWS, M. (1992). Local circuits for the control of leg movements in an insect. *Trends Neurosci.* **15**, 226–232.

BYRNE, J. H., BAXTER, D. A., BUONOMANO, D. V., CLEARY, L. J., ESKIN, A., GOLDSMITH, J. R., MCCLENDON, E., NAZIF, F. A., NOEL, F. AND SCHOLZ, K. P. (1990). Neural and molecular bases of nonassociative and associative learning in *Aplysia*. *Ann. N.Y. Acad. Sci.* **627**, 124–149.

CERF, J. A., GRUNDFEST, H., HOYLE, G. AND MCCANN, F. R. (1959). The mechanism of dual responsiveness in muscle fibers of the grasshopper, *Romalea microptera*. *J. gen. Physiol.* **43**, 377–395.

COHEN, J. L., WEISS, K. R. AND KUPFERMAN, I. (1978). Motor control of buccal muscles in *Aplysia*. *J. Neurophysiol.* **41**, 157–180.

COLMAN, H. AND LICHTMAN, J. W. (1993). Interactions between nerve and muscle: synapse elimination at the developing neuromuscular junction. *Dev. Biol.* **156**, 1–10.

DAGAN, D. AND ADAMS, W. B. (1981). Triplicated bursting neuron R15 in an *Aplysia* abdominal ganglion: Non-symmetrical coupling, common synaptic inputs and response to dopamine. *Brain Res.* **208**, 59–65.

DAVIS, N. T., HOMBERG, U., DIRCKSEN, H., LEVINE, R. B. AND HILDEBRAND, J. G. (1993). Crustacean cardioactive peptide-immunoreactive neurons in the hawkmoth *Manduca sexta* and changes in their immunoreactivity during postembryonic development. *J. comp. Neurol.* **338**, 612–627.

DAVIS, N. T., VELLEMAN, S. G., KINGAN, T. G. AND KESHISHIAN, H. (1989). Identification and distribution of a proctolin-like neuropeptide in the nervous system of the gypsy moth, *Lymantria dispar* and in other Lepidoptera. *J. comp. Neurol.* **283**, 71–85.

DIETMER, J. W. (1977). Electrical properties of skeletal muscle fibers of the flour moth larva, *Ephestia kuehniella*. *J. Insect Physiol.* **23**, 33–38.

DOE, C. Q., SMOUSE, D. AND GOODMAN, C. S. (1988). Control of neuronal fate by the *Drosophila* segmentation gene *even-skipped*. *Nature* **333**, 376–378.

FERGUSON, G. P. AND BENJAMIN, P. R. (1991). The whole-body withdrawal response of *Lymnaea stagnalis*. II. Activation of central motoneurons and muscles by sensory input. *J. exp. Biol.* **158**, 97–116.

HARDIE, J. (1976). Motor innervation of the supercontracting longitudinal ventro-lateral muscles of the blowfly larva. *J. Insect Physiol.* **22**, 661–668.

HINTON, H. E. (1955). On the structure, function and distribution of the prolegs of the Panorpoidea, with a criticism of the Berlese–Imms theory. *Trans. R. ent. Soc. Lond.* **106**, 455–517.

HOYLE, G. (1955). The anatomy and innervation of locust skeletal muscle. *Proc. R. Soc. Lond. B* **143**, 281–292.

HOYLE, G. (1974). Neural control of skeletal muscle. In *The Physiology of Insecta*, vol. 4 (ed. M. Rockstein), pp. 175–236. New York: Academic Press.

JACK, J. J. B., NOBLE, D. AND TSIEN, R. W. (1975). *Electric Current Flow in Excitable Cells*. Oxford: Oxford Scientific Press.

JACOBS, G. A. AND WEEKS, J. C. (1990). Postsynaptic changes at a sensory-to-motoneuron synapse contribute to the developmental

loss of a reflex behavior during insect metamorphosis. *J. Neurosci.* **10**, 1341–1356.

KESHISHIAN, H., CHIBA, A., CHANG, T. N., HALFON, M. S., HARKINS, E. W., JARECKI, J., WANG, L., ANDERSON, M. D., CASH, S., HALPERN, M. E. AND JOHANSEN, J. (1993). Cellular mechanisms governing synaptic development in *Drosophila melanogaster*. *J. Neurobiol.* **24**, 757–787.

KUFFLER, D. P. AND MULLER, K. J. (1974). The properties and connections of supernumerary sensory and motor nerve cells in the central nervous system of an abnormal leech. *J. Neurobiol.* **5**, 331–348.

KUFFLER, D. P., THOMPSON, W. AND JANSEN, J. K. S. (1977). The elimination of synapses in multiply-innervated skeletal muscle fibers of the rat: dependence on distance between end plates. *Brain Res.* **138**, 353–358.

KUTSCH, W. AND BRIEDBACH, O. (1994). Homologous structures in the nervous system of Arthropoda. *Adv. Insect Physiol.* **24**, 1–113.

KUTSCH, W. AND SCHNEIDER, H. (1987). Histological characterization of neurones innervating functionally different muscles of *Locusta*. *J. comp. Neurol.* **261**, 515–528.

KUTSCH, W. AND USHERWOOD, P. N. R. (1970). Studies of the innervation and electrical activity of flight muscles in the locust, *Schistocerca gregaria*. *J. exp. Biol.* **52**, 299–312.

LEVINE, R. B. AND TRUMAN, J. W. (1985). Dendritic reorganization of abdominal motoneurons during metamorphosis of the moth, *Manduca sexta*. *J. Neurosci.* **5**, 2424–2431.

LEVINE, R. B. AND WEEKS, J. C. (1990). Hormonally mediated changes in simple reflex circuits during metamorphosis in *Manduca*. *J. Neurobiol.* **21**, 1022–1036.

LNENICKA, G. A. AND MURPHEY, R. K. (1989). The refinement of invertebrate synapses during development. *J. Neurobiol.* **20**, 339–355.

MENDELL, L. M. AND HENNEMAN, E. (1971). Terminals of single Ia fibers: location and distribution within a pool of 300 homonymous motoneurons. *J. Neurophysiol.* **34**, 171–187.

MILES, C. I. AND WEEKS, J. C. (1991). Developmental attenuation of the pre-ecdysis motor pattern in the tobacco hornworm, *Manduca sexta*. *J. comp. Physiol.* A **168**, 179–190.

MITANI, S., DU, H., HALL, D. H., DRISCOLL, M. AND CHALFIE, M. (1993). Combinatorial control of touch receptor neuron expression in *Caenorhabditis elegans*. *Development* **119**, 773–783.

NOVICKI, A. AND WEEKS, J. C. (1993). Organization of the larval pre-ecdysis motor pattern in the tobacco hornworm, *Manduca sexta*. *J. comp. Physiol.* A **173**, 151–162.

NUDELL, B. M. AND GRINNELL, A. D. (1983). Regulation of synaptic position, size and strength in anuran skeletal muscle. *J. Neurosci.* **3**, 161–176.

PETERSON, B. A. AND WEEKS, J. C. (1988). Somatotopic mapping of sensory neurons innervating mechanosensory hairs on the larval prolegs of *Manduca sexta*. *J. comp. Neurol.* **275**, 128–144.

PFLÜGER, H.-J., WITTEN, J. L. AND LEVINE, R. B. (1993). Fate of abdominal ventral unpaired median (VUM) cells during metamorphosis of the tobacco hawkmoth, *Manduca sexta*. *J. comp. Neurol.* **335**, 508–522.

PICHON, Y. AND ASHCROFT, F. M. (1985). Nerve and muscle: electrical activity. In *Comprehensive Insect Physiology, Biochemistry and Pharmacology*, vol. 5 (ed. G. A. Kerkut and L. I. Gilbert), pp. 85–113. New York: Pergamon.

QUICKE, D. L. J. AND BRACE, R. C. (1979). Differential staining of cobalt- and nickel-filled neurones using rubeanic acid. *J. Microscopy* **115**, 161–163.

RALL, W. (1969). Time constants and electrotonic length of membrane cylinders and neurons. *Biophys. J.* **9**, 1483–1508.

RHEUBEN, M. B. (1972). The resting potential of moth muscle fibre. *J. Physiol., Lond.* **255**, 529–554.

RHEUBEN, M. B. AND KAMMER, A. E. (1983). Mechanisms influencing the amplitude and time course of the excitatory junction potential. In *The Physiology of Excitable Cells* (ed. A. D. Grinnell and W. Moody), pp. 393–409. New York: Alan R. Liss Inc.

ROBERTSON, R. M. (1990). Synchronous activity of flight neurons in the mesothoracic ganglion of the locust. *J. comp. Physiol.* A **167**, 61–69.

SANDSTROM, D. J. (1993). Respecification of identified larval muscles, motoneurons and interneurons to pupal functions in *Manduca sexta*. PhD dissertation, University of California, Berkeley.

SANDSTROM, D. J. AND WEEKS, J. C. (1991*a*). Reidentification of larval interneurons in the pupal stage of *Manduca sexta*. *J. comp. Neurol.* **308**, 311–327.

SANDSTROM, D. J. AND WEEKS, J. C. (1991*b*). Segment-specific fates of proleg muscles and motoneurons during metamorphosis in *Manduca sexta*. *Soc. Neurosci. Abstr.* **17**, 1227.

SIEGLER, M. V. S. (1982). Electrical coupling between supernumerary motor neurons in the locust. *J. exp. Biol.* **101**, 105–119.

SINGH, S. AND WU, C. F. (1990). Properties of potassium currents and their role in membrane excitability in *Drosophila* larval muscle fibers. *J. exp. Biol.* **152**, 59–76.

SNEDECOR, G. W. AND COCHRAN, W. G. (1980). *Statistical Methods*. Ames, Iowa: Iowa State University Press.

SONEA, I. M. AND RHEUBEN, M. B. (1992). Degenerative changes in the function of neuromuscular junctions of *Manduca sexta* during metamorphosis. *J. exp. Biol.* **167**, 61–89.

STEEVES, J. D. AND PEARSON, K. G. (1983). Variability in the structure of an identified interneurone in isogenic clones of locusts. *J. exp. Biol.* **103**, 47–54.

STREICHERT, L. C. AND WEEKS, J. C. (1994). Selective death of identified *Manduca sexta* motoneurons is induced by ecdysteroids *in vitro*. *Soc. Neurosci. Abstr.* **20**, 461.

STREICHERT, L. C. AND WEEKS, J. C. (1995). Decreased monosynaptic input to an identified motoneuron is associated with steroid-mediated dendritic regression during metamorphosis in *Manduca sexta*. *J. Neurosci.* **15**, 1484–1495.

TAYLOR, H. M. AND TRUMAN, J. W. (1974). Metamorphosis of the abdominal ganglia of the tobacco hornworm, *Manduca sexta*. *J. comp. Physiol.* **90**, 367–388.

THORN, R. S. AND TRUMAN, J. W. (1989). Sex-specific neuronal respecification during the metamorphosis of the tobacco hornworm, *Manduca sexta*. *J. comp. Neurol.* **284**, 489–503.

TREISTMAN, S. N. (1979). Duplication of a spontaneously active neuron in *Aplysia*, electrical coupling and effects of a phosphodiesterase inhibitor. *J. Neurobiol.* **10**, 325–330.

TREISTMAN, S. N. AND SCHWARTZ, J. H. (1976). Functional constancy in *Aplysia* nervous systems with anomalously duplicated identified neurons. *Brain Res.* **109**, 607–614.

TRIMMER, B. A. AND WEEKS, J. C. (1989). Effects of nicotinic and muscarinic agents on an identified motoneurone and its direct afferent inputs in larval *Manduca sexta*. *J. exp. Biol.* **144**, 303–337.

TRIMMER, B. A. AND WEEKS, J. C. (1993). Muscarinic acetylcholine receptors modulate the excitability of an identified insect motoneuron. *J. Neurophysiol.* **69**, 1821–1836.

WALDROP, B. AND LEVINE, R. B. (1989). Development of the gin trap reflex in *Manduca sexta*: a comparison of larval and pupal motor responses. *J. comp. Physiol.* A **165**, 743–753.

WALKER, H. M. AND LEV, J. (1953). *Statistical Inference*. New York: Holt.

WATSON, A. H. D., BURROWS, M. AND HALE, J. P. (1985). The morphology and ultrastructure of common inhibitory motor neurones in the thorax of the locust. *J. comp. Neurol.* **239**, 341–359.

WEEKS, J. C. AND DAVIDSON, S. K. (1994). Influence of interganglionic interactions on steroid-mediated dendritic reorganization and death of proleg motor neurons during metamorphosis in *Manduca sexta*. *J. Neurobiol.* **25**, 535–554.

WEEKS, J. C., DAVIDSON, S. K. AND DEBU, B. H. G. (1993). Effects of a protein synthesis inhibitor on the hormonally-mediated regression and death of motoneurons in the tobacco hornworm, *Manduca sexta. J. Neurobiol.* **24**, 125–140.

WEEKS, J. C. AND ERNST-UTZSCHNEIDER, K. (1989). Respecification of larval proleg motoneurons during metamorphosis of the tobacco hornworm, *Manduca sexta*: segmental dependence and hormonal regulation. *J. Neurobiol.* **20**, 569–592.

WEEKS, J. C. AND JACOBS, G. A. (1987). A reflex behavior mediated by monosynaptic connections between hair afferents and motoneurons in the larval tobacco hornworm, *Manduca sexta*. *J. comp. Physiol.* A **160**, 315–329.

WEEKS, J. C., JACOBS, G. A., PIERCE, J. T., SANDSTROM, D. J., STREICHERT, L. C., TRIMMER, B. A., WIEL, D. E. AND WOOD, E. R. (1996). Neural mechanisms of behavioral plasticity: metamorphosis and learning in *Manduca sexta*. *Brain Behav. Evol*. (in press).

WEEKS, J. C., ROBERTS, W. M. AND TRIMBLE, D. L. (1992). Hormonal regulation and segmental specificity of motoneuron phenotype during metamorphosis of the tobacco hornworm, *Manduca sexta*. *Dev. Biol.* **149**, 185–196.

WEEKS, J. C. AND TRUMAN, J. W. (1984*a*). Neural organization of peptide-activated ecdysis behaviors during the metamorphosis of *Manduca sexta*. II. Retention of the proleg motor pattern despite loss of the prolegs at pupation. *J. comp. Physiol.* A **155**, 423–433.

WEEKS, J. C. AND TRUMAN, J. W. (1984*b*). Neural organization of peptide-activated ecdysis behaviors during the metamorphosis of *Manduca sexta*. I. Conservation of the peristalsis motor pattern at the larval–pupal transformation. *J. comp. Physiol.* A **155**, 407–422.

WEEKS, J. C. AND TRUMAN, J. W. (1985). Independent steroid control of the fates of motoneurons and their muscles during insect metamorphosis. *J. Neurosci.* **5**, 2290–2300.

WHITINGTON, P. M. (1985). Functional connections with foreign muscles made by a target-deprived motoneuron. *Dev. Biol.* **107**, 537–540.

WINE, J. J. AND KRASNE, F. B. (1982). The cellular organization of crayfish escape behavior. In *The Biology of Crustacea*, vol. 4 (ed. D. C. Sandeman and H. L. Atwood), pp. 241–292. New York: Academic Press.